LAWRENCE
LIVERMORE
NATIONAL
LABORATORY

LLNL-JRNL-411366

(n,2n) and (n,3n) cross sections of neutron-induced reactions on 150Sm for En from threshold to 35 MeV

D. Dashdorj, G. Mitchell, T. Kawano, J. Becker, C.-Y. Wu, M. Devlin, N. Fotiades, R. Nelson, S. Kunieda

March 18, 2009

Nuclear Inst. and Methods in Physics Research B

Disclaimer

(n,2n) and (n,3n) cross sections of neutron-induced reactions on ^{150}Sm for E_n from threshold to 35 MeV

Dugersuren Dashdorj[1,2,3]*, Gary E. Mitchell[1,4], Toshihiko Kawano[5], John A. Becker[3], Ching-Yen Wu[3], Matt Devlin[5], Nikolaos Fotiades[5], Ronald O. Nelson[5], and Satoshi Kunieda[6]

[1] *North Carolina State University, Raleigh, NC 27695 U.S.A.*

[2] *MonAme Scientific Research Center, Ulaanbaatar, Mongolia*

[3] *Lawrence Livermore National Laboratory, Livermore, CA 94551 U.S.A*

[4] *Triangle Universities Nuclear Laboratory, Durham, NC U.S.A. 27708*

[5] *Los Alamos National Laboratory, Los Alamos, NM 87545 U.S.A.*

[6] *Japan Atomic Energy Agency, Tokai, Ibaraki 319-1195, Japan*

Abstract

Cross-section measurements were made of prompt discrete γ-ray production as a function of incident neutron energy (E_n = 1 to 35 MeV) on a ^{150}Sm sample of 1550 mg/cm^2 of Sm_2O_3 enriched to 95.6% in ^{150}Sm. Results are compared with enhanced Hauser-Feshbach model calculations including the pre-equilibrium reactions. Energetic neutrons were delivered by the Los Alamos Neutron Science Center facility. The prompt-reaction γ rays were detected with the Compton-suppressed Germanium Array for Neutron Induced Excitations (GEANIE). Incident neutron energies were determined by the time-of-flight technique. Excitation functions for thirteen individual γ-rays up to E_x = 0.8 MeV in ^{149}Sm and

one γ-ray transition between the first excited and ground state in ^{148}Sm were measured.

Partial γ-ray cross sections were calculated using GNASH, an enhanced Hauser-Feshbach statistical nuclear reaction model code, and compared with the experimental results. The particle transmission coefficients were calculated with new systematic "global" optical model potential parameters. The coupled-channel optical model based on the soft rotor model was employed to calculate the particle transmission coefficients. The pre-equilibrium part of the spin distribution in ^{150}Sm was calculated using the quantum mechanical theory of Feshbach, Kerman, and Koonin (FKK) and incorporated into the GNASH reaction model code. The partial cross sections for discrete γ-ray cascade paths leading to the ground state in ^{149}Sm and ^{148}Sm have been summed (without double counting) to estimate lower limits for reaction cross sections. These lower limits are combined with Hauser-Feshbach model calculations to deduce the reaction channel cross sections. These reaction channel cross sections agree with previously measured experimental and ENDF/B-VII evaluations.

KEYWORDS: ***γ-ray production cross section, reaction mechanism, GEANIE, neutron induced reaction cross sections, statictical reaction code, samarium***

*Corresponding author, E-mail: ddashdo@ncsu.edu

I. Introduction

The understanding of neutron-induced reactions is an important step in the continued development of nuclear reaction modeling. Also, accurate measurements of neutron-induced cross section data on structural materials and rare earth metals has many applications. For example design of next generation nuclear reactors such as fast reactors require precise cross section data for higher incident neutron energies because fast reactors use higher energy neutrons to initiate fission.

Recent results from studies of γ-ray production cross section measurements from energetic neutron-induced reactions at LANSCE performed with the GEANIE detector array[1] demonstrated that the pre-equilibrium reaction mechanism with its characteristic spin distribution has a large impact on γ-ray production when incident neutron energies are above 8 MeV.[2,3] Semiclassical theories such as the exciton model[4] generally predict the correct split between the Compound Nucleus and Pre-equilibrium contributions to the reaction mechanism. However the traditional assumption is that the two reaction pieces have the same (compound nucleus) spin distribution is not perfect.

Neutron inelastic scattering populates excited states either (1) by forming the compound nucleus and decaying by neutron emission, or (2) by the incoming neutron transferring energy to create a particle-hole pair, and thus initiating the pre-equilibrium process. These two processes produce rather different spin distributions – the momentum transfer via the pre-equilibrium process tends to be smaller than in the compound reaction. This difference in the spin population has a significant impact on the de-excitation γ-ray cascade, favoring lower spin state population at the expense of higher spin states. The realistic treatment of the spin distribution included here improved the accuracy of calculations of

γ-ray production cross sections with the statistical Hauser-Feshbach model.[3)]

The spin-distribution in the pre-equilibrium process is calculated with the FKK model, and the calculated spin-distribution is combined with the GNASH Hauser-Feshbach statistical model calculations.[5)] We used a newly developed "global" optical model potential which was obtained by systematic coupled-channels analysis on medium and heavy nuclei. It was difficult to obtain the local potentials for Sm isotopes due to lack of experimental data for both total and elastic scattering cross sections. We employed a coupled-channel optical model based on the soft rotator model.

In the present work partial n + ^{150}Sm reaction γ-ray cross sections were measured. Energetic neutrons were produced using the spallation neutron beam and the γ-ray spectroscopy was accomplished with the Compton suppressed germanium detector array (GEANIE). The experiment was performed at the WNR branch of the Los Alamos Neutron Science Center (LANSCE). The majority of the known γ-ray transitions in low-lying discrete levels of the residual nucleus have been observed in the (n,n$'$), (n,2n), and (n,3n) channels, and their γ-ray yields have been determined. The individual partial γ-ray cross sections leading to the ground state in the cascade have been combined (without double counting) to produce the experimental lower limit of the ^{150}Sm(n,2nγ)^{149}Sm and ^{150}Sm(n,3nγ)^{148}Sm cross sections. Statistical Hauser-Feshbach model code GNASH predictions of the partial γ-ray cross sections in these reaction channels, with pre-equilibrium spin distributions calculated using FKK theory, are compared with experimental data. The main results presented here are: (i) Experimentally measured partial γ-ray production cross sections in the (n,2n) and (n,3n) reaction channels, (ii) Extracted (n,2n) and (n,3n) reaction channel cross sections and comparisons with previous measurements (if any) and evaluated data. The results are presented in section IV.

II. Experimental setup and data analysis

The experimental data were obtained at the LANSCE Weapons Neutron Research (WNR) facility. At the WNR facility, energetic neutrons are produced by bombarding a natural W target with an 800-MeV pulsed proton beam from the LANSCE linac. The pulsed proton beam consisted of micropulses 1.8 μs (3.6 μs) apart, bunched into macropulses 625 μs in duration. Spallation neutrons with energies ranging from a few keV to nearly 800 MeV are produced. Beam-hardening material (1.5 cm of lead) was placed in the neutron flight path. The neutrons were collimated to a circular beam spot about 1.5 cm in diameter at the scattering-sample position. The scattering sample consisted of 1550 mg/cm^2 of Sm_2O_3 in the form of disks, enriched to 95.6% in ^{150}Sm. The γ rays were detected with the GEANIE spectrometer, located about 20 m from the neutron source on the WNR 60° right flight path. For this experiment, the GEANIE spectrometer consisted of 11 planar and 15 25% High-purity Ge (HPGe) coaxial detectors. All of the planars and 9 of the coaxial detectors were equipped with Compton suppression shields. The detectors were situated at a distance of $\approx$ 14 cm from the spectrometer focal point where the scattering sample is located. The planar detectors were used to measure γ rays with energies less than 1 MeV and the coaxial detectors to measure γ rays with energies up to 3 MeV. The efficiency of the array has been calibrated by a series of source measurements, supplemented by detailed modeling.[6] A fission chamber consisting of ^{235,238}U foils[7] was located 2 m upstream from the GEANIE spectrometer, and the neutron flux was determined using the ^{238}U fission chamber. Neutron energies were determined by the time-of-flight (TOF) technique, using the detection time of the "flash" of γ rays caused by the spallation reaction as a reference marker. The detection time of the γ rays produced

by neutrons interacting with the sample was used to calculate the TOF of the neutrons relative to the γ-flash detection time. Similarly, signals from the fission chamber were used to provide a flight time relative to the γ-flash detection time (also observed in the fission chamber). More extensive descriptions of the LANSCE/WNR facility and the GEANIE spectrometer are given in reference.[1)]

The data were collected for 10 days with 1.8 μs spacing between micro beam pulses. A total of about 2.4×10^8 single- and higher-fold events were recorded. Partial γ-ray cross sections for the production of discrete γ-rays from the reaction ^{150}Sm(n,2nγ)^{149}Sm for incident energies between threshold and 20 MeV are reported in Ref.[8)] There were also separate experimental runs with a target "sandwiched" between 0.2 mm natural iron foils; thus Sm data could be cross reference with standard the Fe(n,n$'\gamma$) cross section.[9)] There is a neutron "wrap-around" problem at the 1.8 μs micropulse spacing for neutrons populating the ^{150}Sm 334-keV state. The flight path is long enough that low energy neutrons strike the target location at the same time as high-energy neutrons from a successive pulse for the 334-keV level in (n,n$'$) reaction. Therefore the yield of the 334-keV transition between the first excited 2^+ state and the ground state of ^{150}Sm extracted from the 1.8 μs spacing data does not in principle give the correct inelastic scattering cross section for the ^{150}Sm first excited state for E_n below 3.9 MeV. In order to resolve this problem a one-day run with 3.6 μs micropulse spacing was performed. The partial γ-ray cross sections of $^{150}\mathrm{Sm}(n,n'\gamma)^{150}\mathrm{Sm}$ for E_n = 1 – 35 MeV extracted from 3.6 μs spacing data were compared with the 1.8 μs spacing data. The comparisons of two prominent γ-ray cross sections are shown in Fig. 1. Agreement between 1.8 and 3.6 μs micropulse spacing data was good, despite the "wrap-around".

[Fig. 1 about here.]

During data playback, events are separated into beam-on and beam-off matrices and a matrix of E_γ vs. neutron TOF generated. In order to improve the statistics, data from detectors of a particular type (planar or coaxial) were summed without weighting. The energy calibration was performed using the energies of well-known transitions in ^{150}Sm and other isotopes in the beam-on data for each set of detectors. The excitation functions were obtained by applying TOF gates 15 ns wide on the γ-ray events in the interval E_n = 1 to 35 MeV. Partial γ-ray cross sections for transitions were obtained using the following formula

$$\sigma_\gamma(E_n) = (1+\alpha) * \frac{\epsilon_{fc}}{\epsilon_{Ge}} * \frac{LT_{fc}}{LT_{Ge}} * \frac{1}{a_s}\frac{A_\gamma}{N_n}, \quad (1)$$

where α is the internal conversion coefficient, ϵ_{Ge} and ϵ_{fc} are the detection efficiency of the germanium detectors and the fission chamber, LT_{Ge} and LT_{fc} are the live times of the germanium detectors and the fission chamber, a_s is the areal density of the ^{150}Sm sample, A_γ the γ - ray peak area, and N_n the number of neutrons determined from the fission chamber data.

The neutron flux used in Eq. (1) was determined from the ^{238}U(n,f) reactions in the fission chamber. The fragment detection efficiency for the fission detector is $\epsilon_{fc} = 0.97$. The γ-ray absolute efficiency curves for planar and coaxial detectors were calculated for GEANIE data using a Monte-Carlo simulation of the array.[6] The calculated efficiency curves are corrected for beam-profile, target-geometry effects, and calibrated against reference γ-ray sources. The Monte-Carlo simulations for the coaxial detectors were performed for γ ray energies between 300 keV and 1800 keV. The efficiency curve for coaxial detectors was extrapolated to 3 MeV and verified with γ ray reference sources. The deadtime fractions (1 - livetime) in Eq. (1) were calculated from the ratio of measured ADC and

scaler counts. Total deadtimes of 62.0% and 58.0% were determined for the planar and coaxial sums, respectively, and deadtimes of 52.0% and 50.9% were obtained for the ^{235}U and ^{238}U fission foils.

To confirm our experimental and analysis techniques, the partial cross section of the $2_1^+ \rightarrow 0_1^+$ transition (847-keV) in ^{56}Fe was extracted from a series of runs with the ^{150}Sm sample sandwiched between 0.2 mm ^{nat}Fe foils. This partial cross section has been extracted from both planar and coaxial data, and is reported in reference.[8] These data are compared to the cross section of 705 $\pm$ 56 mb at E_n = 14.5 MeV, evaluated by Nelson *et al.*.[9] Good agreement was obtained between the coaxial and planar detectors with the inclusion of a coaxial-correction factor (1.2) that accounts for changes in the solid angles and efficiencies that occurred since the original efficiency calibration. The measured partial cross section for the 847-keV transition was consistent ($\sigma_\gamma(847) = 719 \pm 11$ mb for planar detectors at E_n = 14.5 MeV), with the evaluated value.

Measurements with thick targets require an estimate of multiple-scattering effects. The calculation technique used to obtain the photon-production cross sections with multiple-scattering corrections is described in these references,[10].[11] Multiple-scattering corrections were small for (n,2nγ) and (n,3nγ) reaction channels.

III. Theoretical calculations

The statistical Hauser-Feshbach model code, GNASH was used to calculate the γ-ray production cross sections for neutron inelastic scattering on ^{150}Sm. GNASH calculates the pre-equilibrium process with the exciton model, which is based on semiclassical theory. The exciton model gives the fraction of pre-equilibrium to total particle emission

reasonably well. Here we employ the exciton model for the pre-equilibrium part, but then modify the spin-distribution as calculated with the FKK theory. The one-step calculation of Multi Step Direct (MSD) gives the spin-dependent population of continuum states in ^{150}Sm. Since the ground state spin of ^{150}Sm is zero, the spin distribution in the continuum populated by the one-step process is the same as the J-dependence of the MSD angle-integrated cross sections. The initial population of ^{150}Sm (after neutron inelastic scattering, but before γ-ray cascading) is a sum of pre-equilibrium and compound contributions. The spin-distribution can be calculated on a more realistic basis with the quantum mechanical theory of the pre-equilibrium process. The excited nucleus has a spin-distribution that is peaked at lower J-values when the excitation energy of the residual state is not too high. Thus, e.g., for inelastic neutron scattering the excited state population is expected to favor the lower spin states.[3)]

Precise total-reaction cross sections and particle transmission coefficients should be used for the GNASH computation. ^{150}Sm seems to have rotational-vibrational natures at the low-lying states, since it exists at the middle point of a typical transitional region. Therefore, those values were estimated by the coupled-channels optical model which was based on the soft-rotator model (SRM-CC) for neutrons. The SRM nuclear Hamiltonian parameters were taken from Reference.[12)] These parameters were obtained to reproduce measured data, i.e., low-lying level structure and inelastic scattering cross sections of protons. A global optical model potential was adopted since measured data were very scarce for the total and scattering cross sections. Total and scattering cross sections used for the calculation are in Table 1. The model calculation was done by OPTMAN code coupling major collective levels, i.e, 0_1^+, 0_2^+, 0_4^+, 0_6^+ and 3_1^-.[13)]

[Table 1 about here.]

The level scheme of ^{150}Sm and the γ-ray branching ratios were taken from the Table of Isotopes[14] and RIPL-2.[15] The discrete levels of ^{150}Sm up to 1.836 MeV (8^+) excitation are included in the calculation.

IV. Results and Discussions

1. Partial γ-ray cross sections

The γ-ray transition partial cross sections for n + ^{150}Sm have been measured and analyzed for neutron energies between 1 and 35 MeV. The partial level scheme of the γ-ray cascade in ^{149}Sm is shown in Fig. 2.

[Fig. 2 about here.]

Excitation functions for thirteen individual γ-rays up to E_x = 0.8 MeV in ^{148}Sm and one γ-ray transition between first excited and ground state in ^{148}Sm were measured. Partial γ-ray cross sections for n + ^{150}Sm reactions were calculated using the Hauser-Feshbach code GNASH-FKK for neutron energies up to 35 MeV. The partial γ-ray transition cross sections in the (n,2n) and (n,3n) reaction channels are shown in the Figs. 3 – 5. The partial γ-ray production cross sections in ^{149}Sm of E_γ = 198.6 keV (transition between $11/2^+$ and $9/2^-$ levels), E_γ = 214.8 keV (transition between $13/2^+$ and $11/2^-$ levels), E_γ = 277.1 keV (transition between $5/2^-$ and $7/2^-_{g.s.}$ levels), and E_γ = 281.3 keV (transition between $5/2^-$ and $5/2^-$ levels) are compared with the theoretical model GNASHFKK calculations and shown in Fig 3. The 215-keV γ-ray production cross section has a contamination above E_n = 22 MeV from another 215-keV γ-ray which belongs to ^{147}Sm from (n,4n) reaction channel. Experimentally measured partial γ-ray production cross sections in ^{149}Sm of E_γ = 285.9 keV (transition between $9/2^-$ and $7/2^-_{g.s.}$ levels), E_γ = 461.9 keV

(transition between $13/2^-$ and $5/2^-$ levels), $E_\gamma = 636.4$ keV (transition between $7/2^-$ and $7/2^-_{g.s.}$ levels), and $E_\gamma = 664.0$ keV (transition between $11/2^-$ and $7/2^-_{g.s.}$ levels) are compared with the theoretical model GNASHFKK calculations and shown in Fig. 4. Also the measured partial γ-ray production cross section in ^{148}Sm of $E_\gamma = 550.3$ keV, which is the transition from first excited state of ^{148}Sm to ground state, is compared with the theoretical model GNASHFKK calculations. This $2^+_1 \rightarrow 0^+_{g.s.}$ transition represent almost all of the (n,3n) reaction cross section. Since the emitted γ rays from all decaying cascades proceed through this transition. Overall agreement between measured and calculated individual cross sections are generally very good.

[Fig. 3 about here.]

[Fig. 4 about here.]

[Fig. 5 about here.]

2. (n,2n) and (n,3n) reaction channel cross sections

Measured γ-ray transitions going to ground state and first excited state ($5/2^-$, $E_l = 22.5$ keV) are summed without double counting. Individual transitions leading to ground state are summed to determine the lower limit of the (n,2nγ) cross section. The 277-keV, 254-keV, 285-keV, 350-keV, 327-keV, 590-keV, 636-keV, and 664-keV γ-ray production cross sections are summed.

$$\sigma(n,2n\gamma) \equiv \sigma_\gamma(277)+\sigma_\gamma(254)+\sigma_\gamma(285)+\sigma_\gamma(350)+\sigma_\gamma(327)+\sigma_\gamma(590)+\sigma_\gamma(636)+\sigma_\gamma(664). \quad (2)$$

These lower limits were combined with Hauser-Feshbach calculations to produce a model-dependent estimate of the cross sections using the following equation:

$$\sigma_{reaction}^{deduced} = \sum_i \sigma_{\gamma_i}^{measured} \times \frac{\sigma_{reaction}^{calculated}}{\sum_i \sigma_{\gamma_i}^{calculated}}, \quad (3)$$

where $\sigma_{\gamma}^{measured}$ is measured with GEANIE, and $\sigma_{\gamma}^{calculated}$ is calculated using the GNASH-FKK code. The results are shown in Fig. 6 and tabulated in Table 2.

[Fig. 6 about here.]

[Table 2 about here.]

The deduced ^{150}Sm(n,3n)^{148}Sm cross section results based on the one transition between the first excited state and the ground state are obtained in the same manner as for the (n,2n) reaction channel cross sections, and are shown in Fig. 7 and tabulated in Table 3.

[Fig. 7 about here.]

[Table 3 about here.]

V. Conclusion

Excitation functions of prompt γ rays produced in the n + ^{150}Sm reaction have been measured using the GEANIE spectrometer at the LANSCE/WNR facility. The individual γ-ray yields were converted to partial γ-ray cross sections as a function of incident neutron energy, by accounting for neutron flux, sample thickness, deadtime corrections, detector and fission chamber efficiencies, and internal conversion processes. The spin distribution of the pre-equilibrium process in ^{150}Sm + n reactions was calculated using the quantum mechanical theory of FKK. The FKK spin distribution was incorporated into GNASH calculations and the γ-ray production cross sections were calculated and compared with

experimental data. Spin distributions shift to lower spin values when calculated with the FKK formulation than with the Compound Nuclear predictions. The measured partial γ-ray cross sections reflect this spin difference, since the population of high spin states is suppressed. The quantum mechanical calculation results agree with measured data. Realistic treatment of the spin distribution improves the accuracy of calculations of γ-ray production cross sections.

Lower limits on the ^{150}Sm(n,2nγ)^{149}Sm and ^{150}Sm(n,3nγ)^{148}Sm reaction channel cross sections from the measured data are obtained by summing the partial γ-ray cross sections for transitions directly populating the ground state. These limits are combined with Hauser-Feshbach calculations to estimate the reaction channel cross sections. These (n,2n) and (n,3n) reaction channel cross sections are compared with previously measured data. The (n,2n) reaction channel cross sections are in good agreement with previously measured data and are extended to higher neutron energies. The (n,3n) reaction cross sections are obtained for the first time and compared with the evaluated data.

VI. Acknowledgments

This work was supported by in part by the U.S. Department of Energy Grants No. DE-FG52-06NA26194 and No. DE-FG02-97-ER41042, work performed in part under the auspices of the U.S. Department of Energy by Livermore National Security, LLC, Lawrence Livermore National Laboratory under contract No. DE-AC52-06NA4464, and work performed in part under auspices of the U.S. Department of Energy by Los Alamos National Security, LLC, Los Alamos National Laboratory under contract No. DE-AC52-06NA25396. This work has benefited from the use of the LANSCE accelerator facility,

supported under DOE contract No. DE-AC52-06NA25396.

This work performed under the auspices of the U.S. Department of Energy by Lawrence Livermore National Laboratory under Contract DE-AC52-07NA27344.

References

1) J. A. Becker, R. O. Nelson, "New Physics Opportunities with GEANIE at LANSCE/WNR", *Nucl. Phys. News Int.*, **7**[2], p.11, 1997.

2) T. Kawano, P. Talou, M.B. Chadwick, "Production of isomers by neutron-induced inelastic scattering on ^{193}Ir and influence of spin distribution in the pre-equilibrium process", *Nucl. Instr. Methods Phys. Res.*,**A 562**, 774 (2006).

3) D. Dashdorj, T. Kawano, P. E. Garrett, J. A. Becker, U. Agvaanluvsan, L. A. Bernstein, M. B. Chadwick, M. Devlin, N. Fotiades, G. E. Mitchell, R. O. Nelson, W. Younes, "Effect of Preequilibrium Spin Distribution on ^{48}Ti + n cross sections", *Phys. Rev.* **C 75**, 054612 (2007).

4) E. Gadioli, P.E. Hodgson, *Pre-Equilibrium Nuclear Reactions*, Clarendon Press, Oxford (1992).

5) P.G. Young, E.D. Arthur, M.B. Chadwick, "Comprehensive Nuclear Model Calculations: Theory and Use of the GNASH Code", LA-UR-96-3739, Los Alamos National Laboratory, (1996).

6) D. P. McNabb, D. E. Archer, J. A. Becker, *et al.*, " Uncertainty Budget and Efficiency Analysis for the ^{239}Pu(n,2nγ) Partial Reaction Cross-Section Measurements", UCRL-ID-139906, Lawrence Livermore National Laboratory, (2000).

7) S. A. Wender, S. Balestrini, A. Brown, R. C. Haight, C. M. Laymon, T. M. Lee, P. W. Lisowski, W. McCorkle, R. O. Nelson, W. Parker, N.W. Hill, "A fission ionization detector for neutron flux measurements at a spallation source", *Nucl. Instrum. Methods Phys. Res.*, **A 336**, 226 (1993).

8) J. R. Cooper, J. A. Becker, D. Dashdorj, F. S. Dietrich, P. E. Garrett, R. Hoffman, W. Younes, R. O. Nelson, M. Devlin, N. Fotiades, "Measurement of ^{150}Sm(n,2nγ)^{149}Sm Cross Sections between Threshold and 20 MeV", UCRL-TR-205760, Lawrence Livermore National Laboratory, (2004).

9) R. O. Nelson, N. Fotiades, M. Devlin, J. A. Becker, P. E. Garrett, W. Younes, "Cross-Section Standards for Neutron-Induced Gamma-Ray Production in the MeV Energy Range", *Proc. Int. Conf.*

Nuclear Data for Science and Technology, Santa Fe, USA, 26 Sep – 1 Oct, p.838 (2004).

10) H. Vonach, A. Pavlik, M. B. Chadwick, R. C. Haight, R. O. Nelson, S. A. Wender, P. G. Young, "^{207,208}Pb(n,xnγ) reactions for neutron energies from 3 to 200 MeV", *Phys. Rev.* **C 50**, 1952 (1994).

11) R. O. Nelson, M. B. Chadwick, A. Michaudon, P. G. Young, "High-Resolution Measurements and Calculations of Photon-Production Cross Sections for ^{16}O(n,xγ) Reactions Induced by Neutrons with Energies Between 4 and 200 MeV", *Nucl. Sci. Eng.*, **138**, 105 (2001).

12) S. Kunieda, *et. al.*, to be published in *J. Nucl. Sci. Technol.* (2009).

13) E. Sh. Sukhovitskii, S. Chiba, O. Iwamoto, K. Shibata, T. Fukahori, G. B. Morogovskij, "Programs OPTMAN and SHEMMAN version 8 (2004)", JAERI-Data/Code 2005-002 (2005).

14) R.B. Firestone, *Table of Isotopes*, Eighth Edition, John Wiley & Sons, Inc. (1998).

15) Reference Input Parameter Library, IAEA-TECDOC-1034, (1998).

16) J. Frehaut, A. Berlin, R. Bois, J. Jary, "Status of (n,2n) Cross Section Measurements at Bruyeres-Le-Chatel", EXFOR data, 20416, (1980).

Table 1 Total and scattering cross sections used for transmission coefficients for ^{150}Sm + n calculation

E_n(MeV)	σ(total)(b)	σ(scattering)(b)
1.0	6.43	2.45
2.0	6.80	2.29
3.0	6.18	2.15
5.0	4.78	2.07
10.0	4.71	2.09

Table 2 ^{150}Sm(n,2n)^{149}Sm reaction cross sections deduced in this experiment. The width of the neutron energy bin is given in the column 2.

E_n(MeV)	ΔE_n(MeV)	σ(b)	$\Delta\sigma$(b)
8.66	0.22	0.14	0.01
9.21	0.24	0.59	0.05
9.81	0.27	0.85	0.05
10.47	0.29	0.99	0.05
11.20	0.33	1.26	0.07
12.01	0.35	1.51	0.07
12.95	0.42	1.58	0.08
13.95	0.45	1.59	0.08
15.09	0.51	1.55	0.08
16.40	0.59	1.46	0.09
17.87	0.66	1.20	0.06
19.52	0.74	0.80	0.04
21.49	0.88	0.54	0.03
23.72	1.04	0.34	0.02
26.34	1.18	0.29	0.02
29.38	1.43	0.25	0.01
33.11	1.72	0.21	0.02

Table 3 ^{150}Sm(n,3n)^{148}Sm reaction channel cross sections.

E_n(MeV)	ΔE_n(MeV)	σ(b)	$\Delta\sigma$(b)
13.95	0.45	0.005	0.001
15.09	0.51	0.048	0.029
16.40	0.59	0.138	0.014
17.87	0.66	0.592	0.060
19.52	0.74	0.977	0.098
21.49	0.88	1.241	0.124
23.72	1.04	1.268	0.126
26.34	1.18	1.127	0.112
29.38	1.43	0.711	0.071
33.11	1.72	0.405	0.040

Figure Captions

Fig. 1. Comparison of the 439-, 505-keV partial γ-ray cross sections of ^{150}Sm(n,n$'\gamma$)^{150}Sm obtained with 3.6 and 1.8 μs spacing.

Fig. 2. Partial level scheme of ^{149}Sm.

Fig. 3. Experimentally measured partial γ-ray production cross sections compared with the theoretical model GNASHFKK calculations for ^{149}Sm of E_γ = 198.6 keV (transition between $11/2^+$ and $9/2^-$ levels), E_γ = 214.8 keV (transition between $13/2^+$ and $11/2^-$ levels), E_γ = 277.1 keV (transition between $5/2^-$ and $7/2^-_{g.s.}$ levels), and E_γ = 281.3 keV (transition between $5/2^-$ and $5/2^-$ levels).

Fig. 4. Experimentally measured partial γ-ray production cross sections compared with the theoretical model GNASHFKK calculations for ^{149}Sm of E_γ = 285.9 keV (transition between $9/2^-$ and $7/2^-_{g.s.}$ levels), E_γ = 461.9 keV (transition between $13/2^-$ and $5/2^-$ levels), E_γ = 636.4 keV (transition between $7/2^-$ and $7/2^-_{g.s.}$ levels), and E_γ = 664.0 keV (transition between $11/2^-$ and $7/2^-_{g.s.}$ levels).

Fig. 5. Experimentally measured partial γ-ray production cross sections compared with the theoretical model GNASHFKK calculations for ^{148}Sm of E_γ = 550.3 keV (transition between 2^+_1 and $0^+_{g.s.}$ levels).

Fig. 6. Deduced cross section for the ^{150}Sm(n,2n)^{149}Sm reaction, compared to

the GNASHFKK predictions, ENDF/B-VII evaluations, and previously measured data.[8,16)]

Fig. 7. Deduced cross section for the ^{150}Sm(n,3n)^{148}Sm reaction, compared to the GNASHFKK prediction and ENDF/B-VII evaluation.

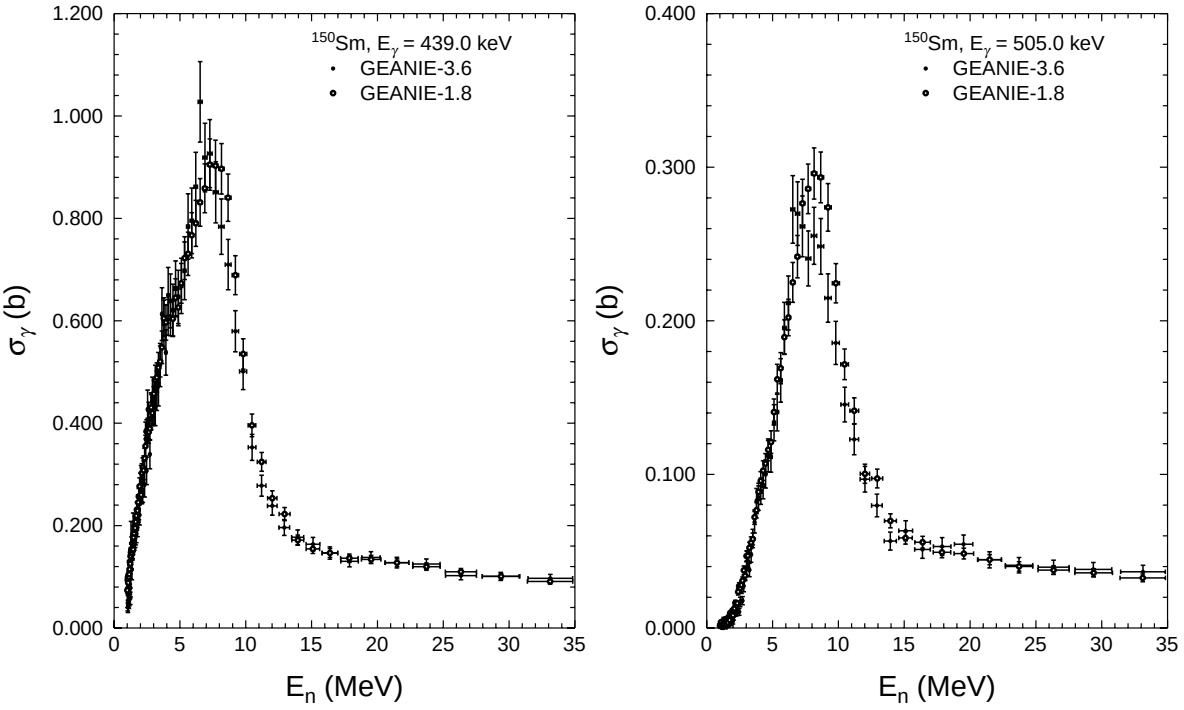

Fig. 1 Comparison of the 439-, 505-keV partial γ-ray cross sections of the ^{150}Sm(n,n$'\gamma$)^{150}Sm reactions obtained with 2 micro pulse spacings, 3.6 and 1.8 microseconds. (•) indicate the 3.6 microsec pulse spacings, (∘) indicate the 1.8 microsec pulse spacings.

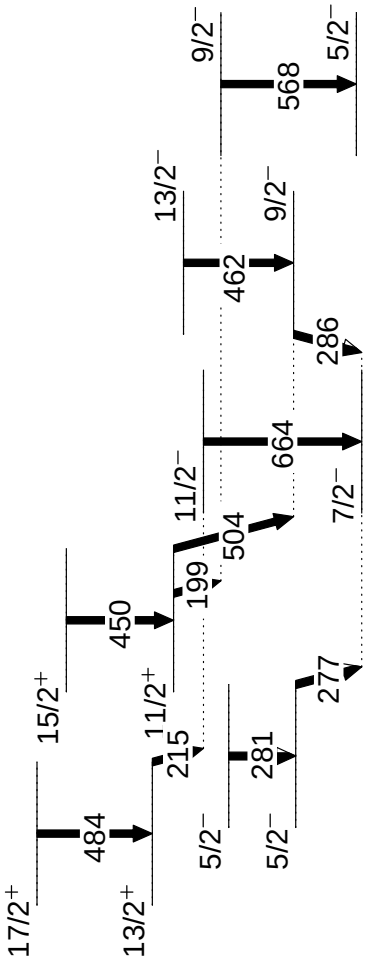

Fig. 2 Partial level scheme of ^{149}Sm (intensity of the γ ray are not to scale).

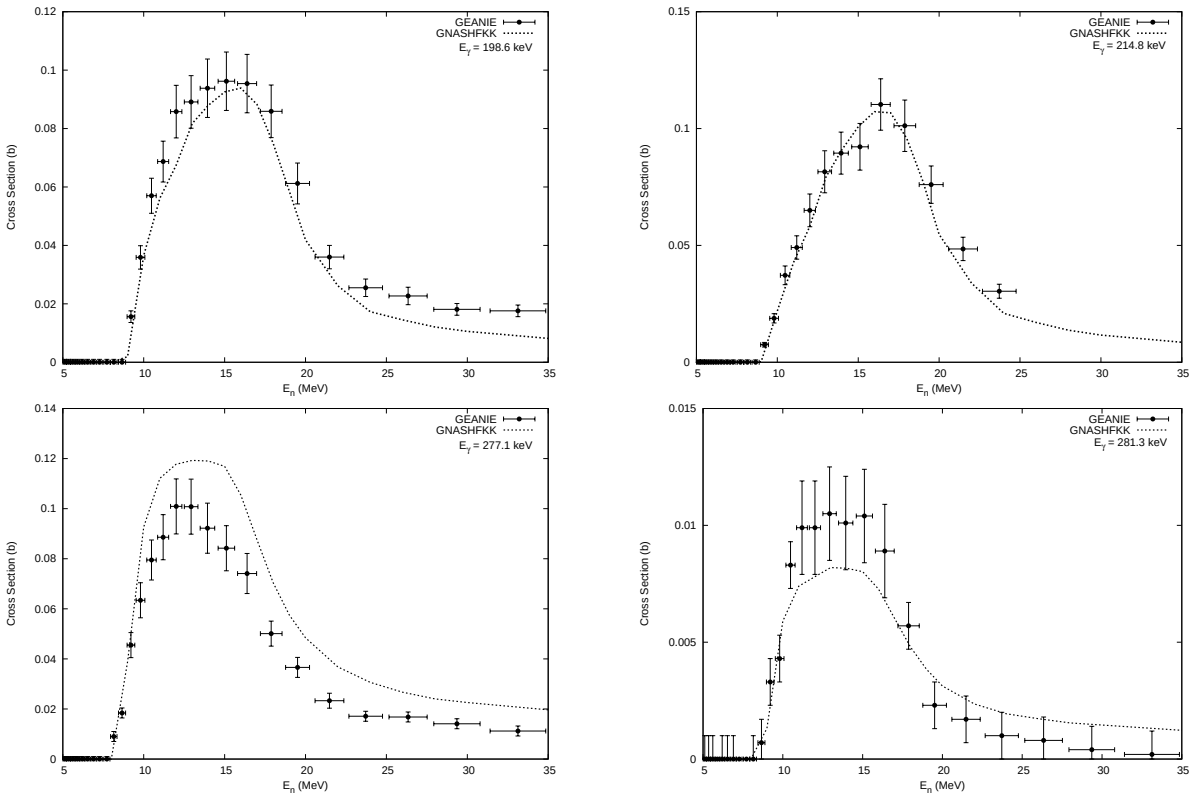

Fig. 3 Experimentally measured partial γ-ray production cross sections compared with the theoretical model GNASHFKK calculations for ^{149}Sm of E_γ = 198.6 keV (transition between $11/2^+$ and $9/2^-$ levels), E_γ = 214.8 keV (transition between $13/2^+$ and $11/2^-$ levels), E_γ = 277.1 keV (transition between $5/2^-$ and $7/2^-_{g.s.}$ levels), and E_γ = 281.3 keV (transition between $5/2^-$ and $5/2^-$ levels).

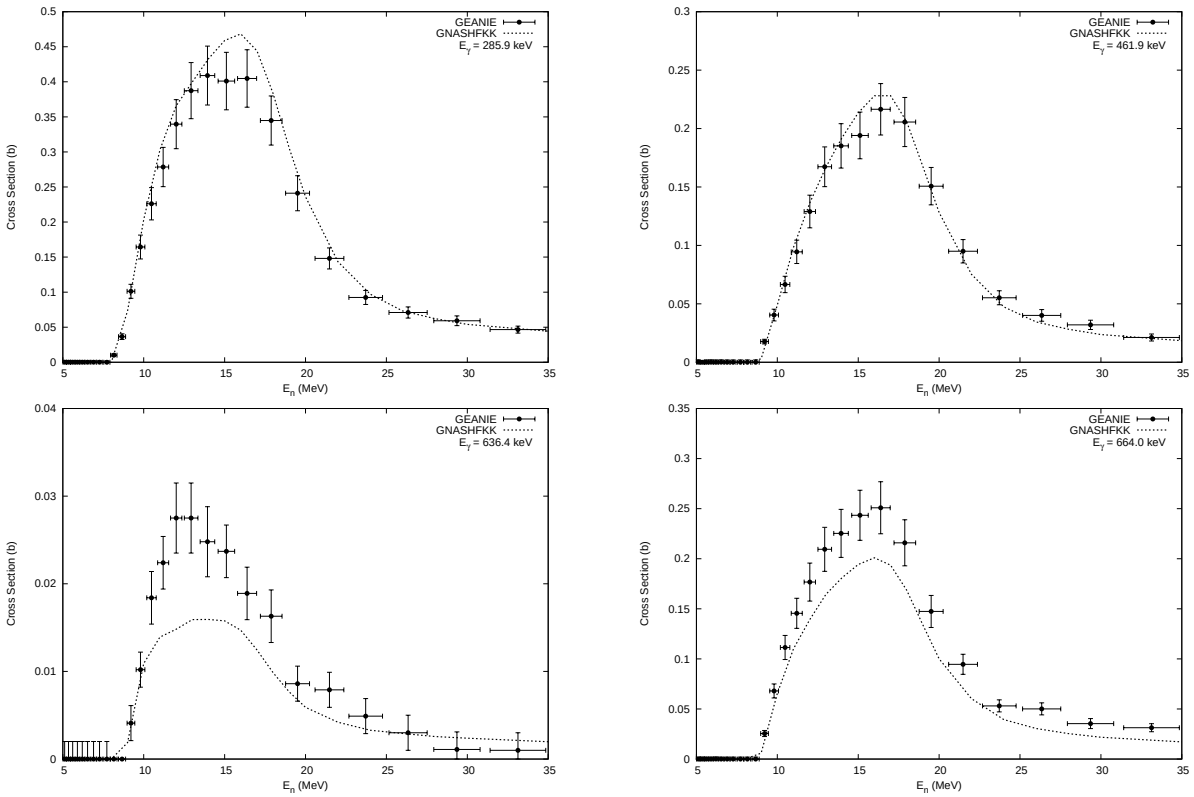

Fig. 4 Experimentally measured partial γ-ray production cross sections compared with the theoretical model GNASHFKK calculations for ^{149}Sm of E_γ = 285.9 keV (transition between $9/2^-$ and $7/2^-_{g.s.}$ levels), E_γ = 461.9 keV (transition between $13/2^-$ and $5/2^-$ levels), E_γ = 636.4 keV (transition between $7/2^-$ and $7/2^-_{g.s.}$ levels), and E_γ = 664.0 keV (transition between $11/2^-$ and $7/2^-_{g.s.}$ levels).

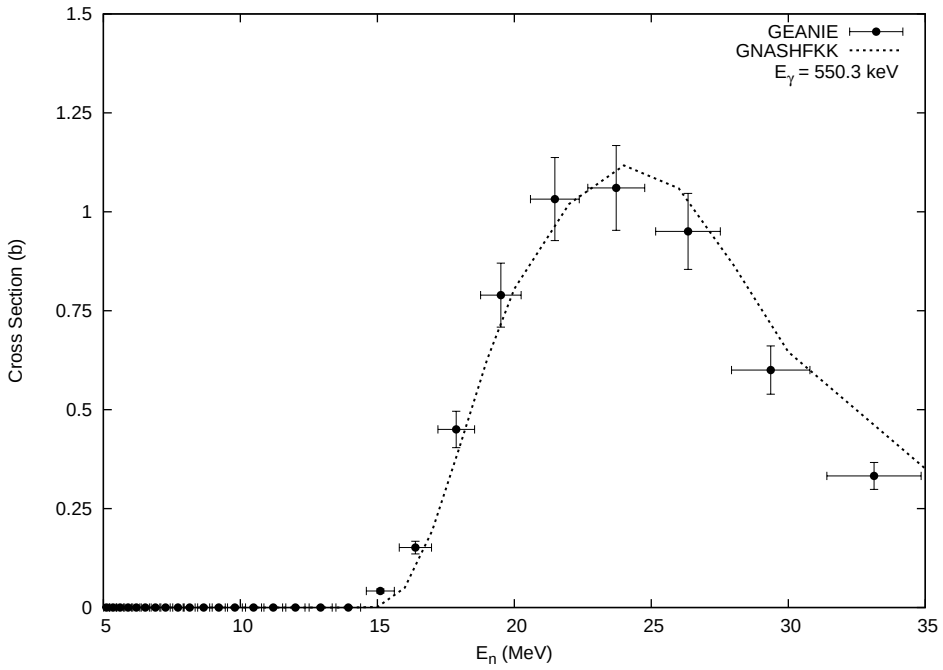

Fig. 5 Experimentally measured partial γ-ray production cross sections compared with the theoretical model GNASHFKK calculations for ^{148}Sm of $E_\gamma = 550.3$ keV (transition between 2_1^+ and $0_{g.s.}^+$ levels).

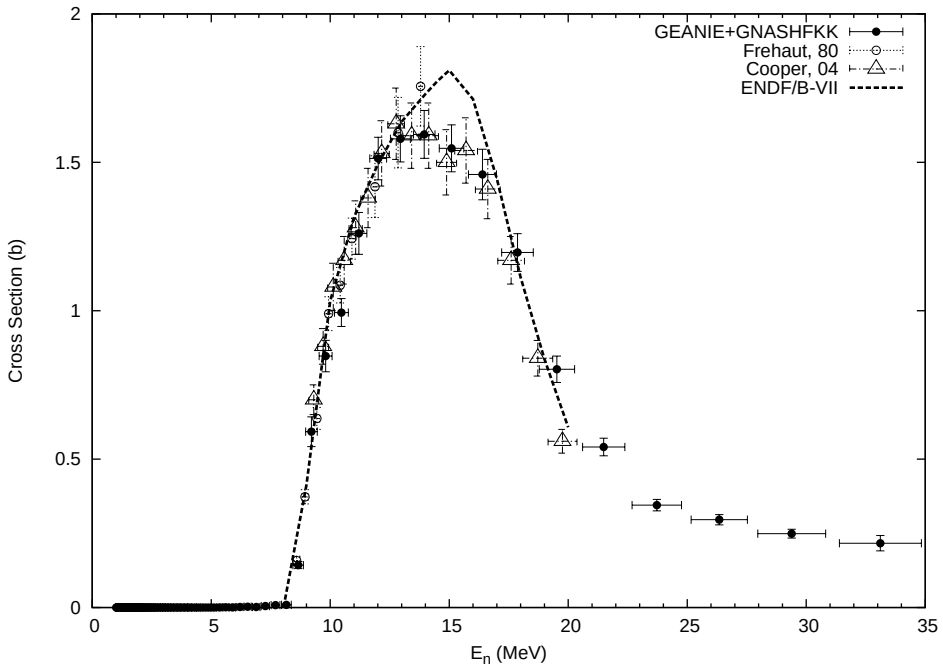

Fig. 6 Deduced cross section for the ^{150}Sm(n,2n)^{149}Sm reaction, compared to the GNASHFKK predictions, ENDF/B-VII evaluations, and previously measured data.[8, 16)]

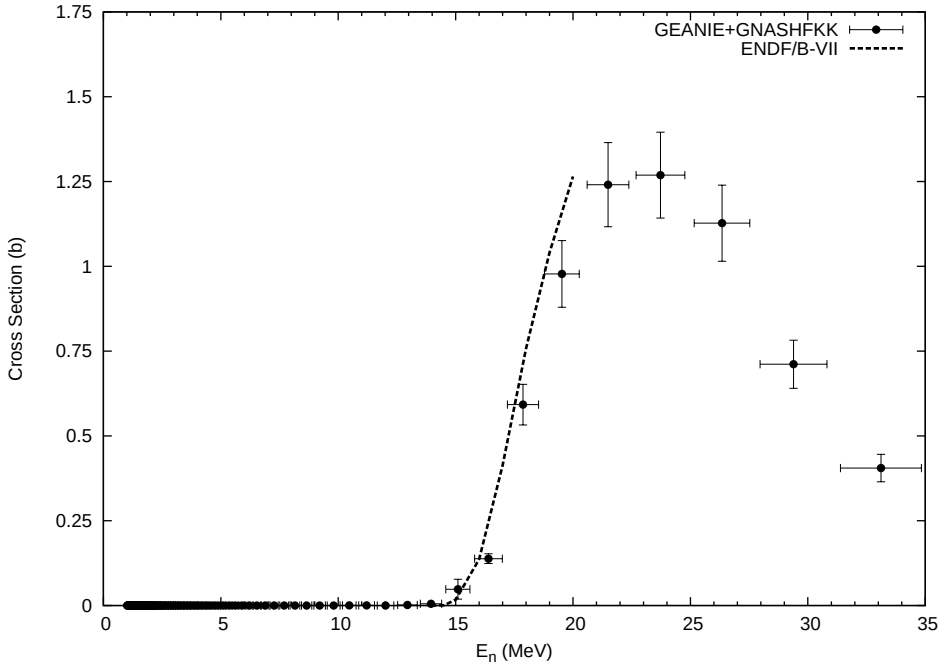

Fig. 7 Deduced cross section for the ^{150}Sm(n,3n)^{148}Sm reaction, compared to the GNASHFKK prediction and ENDF/B-VII evaluation.